# Heading Accuracy Improvement of MEMS IMU/DGPS Integrated Navigation System for Land Vehicle

Dongqing Gu, Naser El-Sheimy
Department of Geomatics Engineering, University of Calgary, Calgary, AB CANADA

*Abstract*-**Many researches indicated that in land vehicle-based MEMS IMU/DGPS integrated navigation system, the vehicle heading is unobservable and its error can grow significantly fast with time, if the vehicle moves with only slow changes in attitude and acceleration, e.g. the vehicle moving along a straight road at almost constant velocity. In this paper, a new heading measurement is derived from the DGPS positions and this new measurement can improve the heading accuracy of MEMS IMU/DGPS integrated navigation system for land vehicle. However, the DGPS-derived heading will have a significant deviation from the true heading value while the vehicle makes a turn. Thus a sequential Kalman filter is proposed to process the DGPS position and heading measurements in a sequential order with MEM IMU measurements. This ensures the DGPS position measurements still can be used in the KF even if the DGPS heading measurements are unusable due to large deviation to the truth. To ensure the quality of the DGPS heading measurements, an innovation detection method is used to detect and reject the singular DGPS heading measurement from the sequential Kalman filter. A field test was conducted to test the effect of this new heading measurement on improving land vehicle heading accuracy. The test results showed that this new type of measurement can significantly reduce the heading error of MEMS IMU/DGPS integrated navigation solution from about 5 deg to less than 1 deg. Test results also showed that the innovation detection method can effectively control the quality of DGPS heading measurement. Without this control, the singular heading measurement would lead to a heading error as large as 100 deg. In summary, the introduction of DGPS-derived new heading measurement and the innovation detection method investigated in this paper can significantly improve the accuracy and reliability of the heading parameter in land vehicle MEMS IMU/DGPS integrated navigation system.**

## I. INTRODUCTION

MEMS inertial measurement unit (IMU) has been widely applied in the navigation system for land vehicle. It is usually integrated with global position system (GPS) to provide the navigation parameters. MEMS IMU can provide high frequency information with good short term accuracy, while GPS can provide low frequency information with excellent long term accuracy. Thus MEMS IMU/GPS integrated navigation system can provide accurate and reliable navigation parameters through optimally synthesizing the information from both MEMS IMU and GPS.

The positioning accuracy of the differential GPS (DGPS) measurement can reach centimeter-level. MEMS IMU integrated by DGPS can provide the accurate velocity and position solution when the DGPS position measurement is available. But there is not always the case for the attitude estimation in the MEMS IMU/DGPS integrated navigation system. When the changes in attitude and velocity are slow, the attitude of the vehicle is unobservable with the DGPS position measurement [1]. And the component of MEMS gyro bias in the direction of specific force is not observable [2]. The heading error thus will increase significantly fast with time.

A new method is presented in this paper to address the above problem. When the vehicle moves along a straight road and its attitude and velocity change at a low rate, the vehicle heading can be calculated approximately from the change of DGPS position measurement in short interval. The vehicle heading calculated by the DGPS position can be used as a new measurement to constrain the heading error increasing with time. A sequential Kalman filter is developed to process the DGPS position measurement and the DGPS heading measurement. In order to detect and reject the singular value of the DGPS heading measurement, an innovation detection method is developed in this paper.

The paper is divided into six sections. Section 2 presents the algorithm of calculating the vehicle heading from DGPS positions. The sequential Kalman filter for the integrated navigation is introduced in Section 3. The innovation detection for detecting and rejecting the singular heading measurement is described in Section 4. Section 5 presents the field test result and the conclusion is drawn in Section 6.

## II. DERIVING HEADING FROM DGPS POSITIONS

The difference of the vehicle horizontal positions can be described as follows:

$$\begin{aligned} \delta\lambda_k &\approx (\lambda_k - \lambda_{k-1}) R \cos L_k \\ \delta L_k &\approx (L_k - L_{k-1}) R \end{aligned} \tag{1}$$

where $\lambda_k$ and $L_k$ are the vehicle longitude and latitude at $t_k$, which are obtained from DGPS positioning solutions, $R$ is the radius of the earth which is modeled as a sphere.

When the vehicle moves along a straight road, the relationship between the vehicle's heading and the differences of the horizontal positions between two points is shown in Fig. 1. The vehicle's heading can be calculated by the differences of the horizontal position as follows:

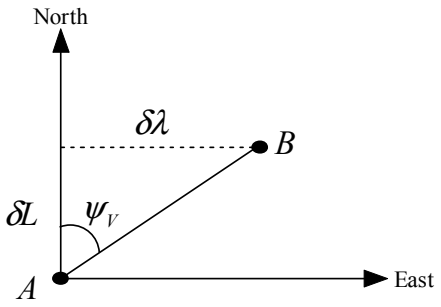


Fig. 1. Vehicle heading.

$$\psi_V = \tan^{-1}\left(\frac{\delta\lambda}{\delta L}\right). \quad (2)$$

The vehicle heading calculated from (2) should be adjusted according to the definition of the heading range. If the heading range is defined from 0 to +/-180 deg, and it is defined that the positive rotation is from north to east and that the negative rotation is from north to west, the vehicle heading calculated from (2) should be adjusted as follows:

$$\begin{cases} \psi_{V_{DGPS}} = \psi_V \text{ , } \delta L > 0 \\ \psi_{V_{DGPS}} = \psi_V + 180 \text{ , } \delta L < 0 \text{ and } \psi_V < 0 \\ \psi_{V_{DGPS}} = \psi_V - 180 \text{ , } \delta L < 0 \text{ and } \psi_V > 0 \end{cases}$$

where the heading unit is degree.

It should be noted that in cases where the vehicle is on turning, the above relationship expressed in Fig. 1 is no longer valid because it is assumed in Fig. 1 that the vehicle is moving in straight and that the vehicle's heading is almost unchanged. Therefore in these cases, the vehicle heading calculated by (2) will have a large deviation from the true vehicle heading, which means the DGPS heading is not useable.

## III. Sequential Kalman Filter For Integrated Navigation

Besides the DGPS position, the vehicle heading derived from the DGPS positions is used as a new measurement in this investigation. As discussed above, the DGPS heading will have large errors and will not be used when vehicle is making turnings, even though the DGPS position is adequately accurate. Considering these situations, the DGPS heading measurements and DGPS position measurements should be processed sequentially so that the DGPS position measurements can still be processed even if the DGPS heading is not available. So the sequential Kalman filter is presented to implement the MEMS IMU/DGPS integrated navigation system.

The state vector of the sequential Kalman filter is as follows:

$$\boldsymbol{X} = \begin{bmatrix} \delta\boldsymbol{r} \\ \delta\boldsymbol{V} \\ \boldsymbol{\varphi} \\ \boldsymbol{b}_g \\ \boldsymbol{b}_a \\ \boldsymbol{S}_g \\ \boldsymbol{S}_a \\ \boldsymbol{\gamma}_g \\ \boldsymbol{\gamma}_a \end{bmatrix} \quad (3)$$

where $\delta\boldsymbol{r}$ is the position error vector; $\delta\boldsymbol{V}$ is the velocity error vector; $\boldsymbol{\varphi}$ is the attitude error vector; $\boldsymbol{b}_g$ and $\boldsymbol{b}_a$ are the bias error vectors of the gyros and accelerometers respectively; $\boldsymbol{S}_g$ and $\boldsymbol{S}_a$ are the scale factor error vectors of the gyros and accelerometers respectively; $\boldsymbol{\gamma}_g$ and $\boldsymbol{\gamma}_a$ are the non-orthogonal error of the gyros and accelerometers respectively. The state space model is as follows:

$$\dot{\boldsymbol{X}} = \boldsymbol{F}\boldsymbol{X} + \boldsymbol{W} \quad (4\text{-a})$$

$$\boldsymbol{Z}_1 = \boldsymbol{H}_1\boldsymbol{X} + \boldsymbol{V}_1 \quad (4\text{-b})$$

$$\boldsymbol{Z}_2 = \boldsymbol{H}_2\boldsymbol{X} + \boldsymbol{V}_2 \quad (4\text{-c})$$

where $\boldsymbol{F}$ is the dynamics matrix; $\boldsymbol{W}$ is the state noise vector; $\boldsymbol{Z}_1$ and $\boldsymbol{Z}_2$ are two measurement vectors; $\boldsymbol{H}_1$ and $\boldsymbol{H}_2$ are the measurement matrixes; $\boldsymbol{V}_1$ and $\boldsymbol{V}_2$ are the measurement noise vectors.

The dynamics matrix is as follows [3]:

$$\boldsymbol{F} = \begin{bmatrix} \boldsymbol{F}_{11} & \mathbf{I} & \mathbf{0} & \mathbf{0} & \mathbf{0} & \mathbf{0} & \mathbf{0} & \mathbf{0} & \mathbf{0} \\ \boldsymbol{F}_{21} & \boldsymbol{F}_{22} & (\boldsymbol{f}^c\times) & \mathbf{0} & \boldsymbol{C}_b^p & \mathbf{0} & \boldsymbol{F}_{27} & \mathbf{0} & \boldsymbol{C}_b^p\boldsymbol{\Gamma}_a \\ \mathbf{0} & \mathbf{0} & \boldsymbol{F}_{33} & -\boldsymbol{C}_b^p & \mathbf{0} & \boldsymbol{F}_{36} & \mathbf{0} & -\boldsymbol{C}_b^p\boldsymbol{\Gamma}_g & \mathbf{0} \\ \mathbf{0} & \mathbf{0} & \mathbf{0} & \boldsymbol{F}_{44} & \mathbf{0} & \mathbf{0} & \mathbf{0} & \mathbf{0} & \mathbf{0} \\ \mathbf{0} & \mathbf{0} & \mathbf{0} & \mathbf{0} & \boldsymbol{F}_{55} & \mathbf{0} & \mathbf{0} & \mathbf{0} & \mathbf{0} \\ \mathbf{0} & \mathbf{0} & \mathbf{0} & \mathbf{0} & \mathbf{0} & \boldsymbol{F}_{66} & \mathbf{0} & \mathbf{0} & \mathbf{0} \\ \mathbf{0} & \mathbf{0} & \mathbf{0} & \mathbf{0} & \mathbf{0} & \mathbf{0} & \boldsymbol{F}_{77} & \mathbf{0} & \mathbf{0} \\ \mathbf{0} & \mathbf{0} & \mathbf{0} & \mathbf{0} & \mathbf{0} & \mathbf{0} & \mathbf{0} & \boldsymbol{F}_{88} & \mathbf{0} \\ \mathbf{0} & \mathbf{0} & \mathbf{0} & \mathbf{0} & \mathbf{0} & \mathbf{0} & \mathbf{0} & \mathbf{0} & \boldsymbol{F}_{99} \end{bmatrix}$$

where $\boldsymbol{F}_{11} = -(\boldsymbol{\omega}_{ec}^c\times)$, $\boldsymbol{F}_{21} = \mathrm{diag}(-\omega_s^2, -\omega_s^2, 2\omega_s^2)$, $\boldsymbol{F}_{33} = -[(\boldsymbol{\omega}_{ie}^c\times) + (\boldsymbol{\omega}_{ec}^c\times)]$, $\boldsymbol{F}_{36} = \boldsymbol{C}_b^p\mathrm{diag}(\boldsymbol{\omega}_{ib}^b)$, $\boldsymbol{F}_{44} = \mathrm{diag}(\boldsymbol{c}_{gb})$, $\boldsymbol{F}_{22} = -[(2\boldsymbol{\omega}_{ie}^c\times) + (\boldsymbol{\omega}_{ec}^c\times)]$, $\boldsymbol{F}_{27} = \boldsymbol{C}_b^p\mathrm{diag}(\boldsymbol{f}^b)$, $\boldsymbol{F}_{55} = \mathrm{diag}(\boldsymbol{c}_{ab})$, $\boldsymbol{F}_{66} = \mathrm{diag}(\boldsymbol{c}_{gs})$, $\boldsymbol{F}_{77} = \mathrm{diag}(\boldsymbol{c}_{as})$,

$\boldsymbol{F}_{88}=\mathrm{diag}(\boldsymbol{c}_{g\gamma})$, $\boldsymbol{F}_{99}=\mathrm{diag}(\boldsymbol{c}_{a\gamma})$, $\boldsymbol{C}_{gb}$, $\boldsymbol{C}_{gb}$, $\boldsymbol{C}_{gb}$, $\boldsymbol{C}_{gb}$, $\boldsymbol{C}_{gb}$ and $\boldsymbol{C}_{gb}$ are the coefficients describing the error models for the gyro bias, accelerometer biases, gyro scale factors, accelerometer scale factors, gyro triad non-orthogonalties and accelerometer triad non-orthogonalities respectively. And $\boldsymbol{\Gamma}_g$ and $\boldsymbol{\Gamma}_a$ can be written as follows:

$$\boldsymbol{\Gamma}_g=\begin{bmatrix}\omega_{iby}^b & \omega_{ibz}^b & 0 & 0 & 0 & 0\\ 0 & 0 & \omega_{ibx}^b & \omega_{ibz}^b & 0 & 0\\ 0 & 0 & 0 & 0 & \omega_{ibx}^b & \omega_{iby}^b\end{bmatrix}$$

$$\boldsymbol{H}_{\psi}=\begin{bmatrix}\dfrac{a_{11}(b_{11}c_{31}+b_{12}c_{32}+b_{13}c_{33})}{a_{11}^2+a_{21}^2}\\ \dfrac{a_{21}(b_{11}c_{31}+b_{12}c_{32}+b_{13}c_{33})}{a_{11}^2+a_{21}^2}\\ \dfrac{-a_{11}(b_{11}c_{11}+b_{12}c_{12}+b_{13}c_{12})-a_{21}(b_{11}c_{21}+b_{12}c_{22}+b_{13}c_{33})}{a_{11}^2+a_{21}^2}\end{bmatrix}^{\mathrm{T}}$$

where $a_{ij}$, $b_{ij}$ and $c_{ij}$ are the $ij$th elements of $\boldsymbol{C}_v^n$, $\boldsymbol{C}_b^v$ and $\boldsymbol{C}_b^n$ respectively.

DGPS position and heading are used as two types of update measurements for the MEMS IMU/DGPS integrated navigation. So the measurement vectors of the sequential Kalman filter should be described as follows:

$$\boldsymbol{Z}_1=\boldsymbol{r}_{MEMS}-\boldsymbol{r}_{DGPS} \tag{5}$$

$$Z_2=\psi_{V_{MEMS}}-\psi_{V_{DGPS}} \tag{6}$$

where $\boldsymbol{r}_{MEMS}$ and $\boldsymbol{r}_{DGPS}$ are the vehicle positions from the MEMS inertial navigation system and DGPS respectively; $\psi_{V_{MEMS}}$ and $\psi_{V_{DGPS}}$ are the vehicle headings from the MEMS IMU and DGPS respectively.

The equations of the sequential Kalman filter are as follows [4]:

$$\hat{\boldsymbol{X}}_{k/k-1}=\boldsymbol{\Phi}_{k/k-1}\hat{\boldsymbol{X}}_{k-1} \tag{7}$$

$$\boldsymbol{P}_{k/k-1}=\boldsymbol{\Phi}_{k/k-1}\boldsymbol{P}_{k-1}\boldsymbol{\Phi}_{k/k-1}^{\mathrm{T}}+\boldsymbol{Q}_{k-1} \tag{8}$$

$$\begin{cases}\boldsymbol{K}_{i,k}=\boldsymbol{P}_{i-1,k}\boldsymbol{H}_{i,k}\left(\boldsymbol{H}_{i,k}\boldsymbol{P}_{i-1,k}\boldsymbol{H}_{i,k}+\boldsymbol{R}_{i,k}\right)^{-1}\\ \hat{\boldsymbol{X}}_{i,k}=\hat{\boldsymbol{X}}_{i-1,k}+\boldsymbol{K}_{i,k}\left(\boldsymbol{Z}_{i,k}-\boldsymbol{H}_{i,k}\hat{\boldsymbol{X}}_{i-1,k}\right)\\ \boldsymbol{P}_{i,k}=\left(\boldsymbol{I}-\boldsymbol{K}_{i,k}\boldsymbol{H}_{i,k}\right)\boldsymbol{P}_{i-1,k}\\ i=1,2,\cdots,r\end{cases} \tag{9}$$

where $r$ is the number of the measurements; $\boldsymbol{\Phi}_{k/k-1}$ is the transformation matrix; $\boldsymbol{Q}_{k-1}$ is the covariance matrix of the state noise; $\boldsymbol{R}_{k-1}$ is the covariance matrix of the measurement noise; and $\hat{\boldsymbol{X}}_{0,k}=\hat{\boldsymbol{X}}_{k/k-1}$, $\boldsymbol{P}_{0,k}=\boldsymbol{P}_{k/k-1}$.

$$\boldsymbol{\Gamma}_a=\begin{bmatrix}f_y^b & f_z^b & 0 & 0 & 0 & 0\\ 0 & 0 & f_x^b & f_z^b & 0 & 0\\ 0 & 0 & 0 & 0 & f_x^b & f_y^b\end{bmatrix}$$

The measurement matrixes $\boldsymbol{H}_1$ and $\boldsymbol{H}_2$ are as follows [3]:

$$\boldsymbol{H}_1=\begin{bmatrix}\mathbf{I} & \mathbf{0} & \left(\boldsymbol{C}_b^n\boldsymbol{l}_{GPS}^b\times\right) & \mathbf{0} & \mathbf{0} & \mathbf{0} & \mathbf{0} & \mathbf{0} & \mathbf{0}\end{bmatrix}$$

$$\boldsymbol{H}_2=\begin{bmatrix}\mathbf{0} & \mathbf{0} & \boldsymbol{H}_{\psi} & \mathbf{0} & \mathbf{0} & \mathbf{0} & \mathbf{0} & \mathbf{0} & \mathbf{0}\end{bmatrix}$$

where $\boldsymbol{l}_{GPS}^b$ is the lever arm from SINS to the GPS antenna. And $\boldsymbol{H}_{\psi}$ can be written as follows:

## IV. Innovation Detection For Rejecting The Singular Heading Measurement

On the assumption that the vehicle moves along a straight road with no or small change in its attitude and velocity, the heading can be calculated accurately by the change of the DGPS position according to equation (2). If the assumption is violated, the calculated heading will be deviating far away from the vehicle's true heading. In order to deal with the occurrence of such a situation, an innovation detection method is presented to detect and reject the singular heading measurement.

The innovation of the heading measurement can be described as follows:

$$v_{2,k}=Z_{2,k}-\boldsymbol{H}_{2,k}\hat{\boldsymbol{X}}_{1,k} \tag{10}$$

where $Z_{2,k}$ is the heading measurement described in equation (6); $\boldsymbol{H}_{2,k}$ is the measurement matrix; $\hat{\boldsymbol{X}}_{1,k}$ is the state estimation after updating by the DGPS position measurement. The criterion used to reject the heading measurement from the sequential Kalman filter is as follows:

*If* $|v_{2,k}|>A_{\max}$, *then reject the heading measurement*

where $A_{\max}$ is the maximum-tolerable value of the innovation.

## V. Field Test

A land vehicle field test was conducted in Calgary in December 2005. A GPS master station was installed on the top of the Engineering Building at the University of Calgary. The test included an MEMS IMU, a GPS receiver (NovAtel OEM4), and a tactical grade IMU (LN200). For evaluation purpose, the tactical grade IMU (LN200) was integrated with

DGPS solutions to generate the reference solution of the trajectory. This reference solution was backward smoothed using an RTS smoother in order to provide a sufficiently accurate reference to evaluate the solution of the MEMS IMU/DGPS system [5]. The trajectory and the velocity of the field test are shown in Fig. 2 and Fig. 3 respectively, where it can be seen that the trajectory includes several segments of straight roads and several turns.

The navigation errors of the MEMS IMU/DGPS integrated navigation system using the DGPS heading measurements and the innovation detection method are shown in Fig. 4. As a comparison, the navigation error of the same integration system without using the DGPS heading measurements is shown in Fig. 5. Since no DGPS heading measurements were used in Fig. 5, there is no requirement of implementing the innovation detection method. To assess the effectiveness of the innovation detection method, the navigation error of the integration solution using the DGPS heading information but without the innovation detection implementation is shown in Fig. 6. The RMS errors of the above three cases for the period from 520250 s to the end of the field test are summarized in Table I.

In Fig. 4, it can be seen that after KF convergence, the heading error of the integration solution with the DGPS heading measurement and the innovation detection is less than 1 deg. In Fig. 5 where no DGPS heading information is used, the heading error of the integration solution can be as large as 5 deg. In Fig. 6 where the DGPS heading measurements were used but without implementing the innovation detection method, the singular heading measurements could lead to significantly large navigation errors. The heading error could reach even 100 deg and the position error also reached 2 meter.

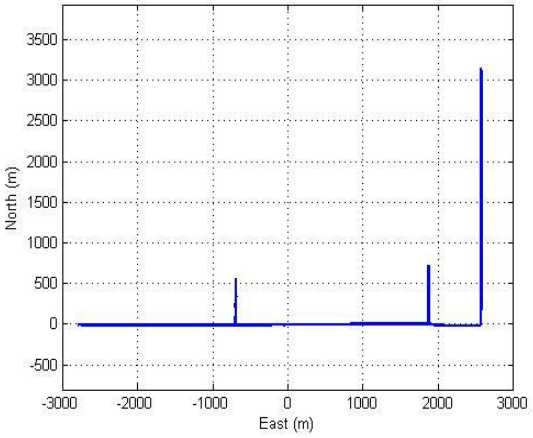


Fig. 2. Field test trajectory.

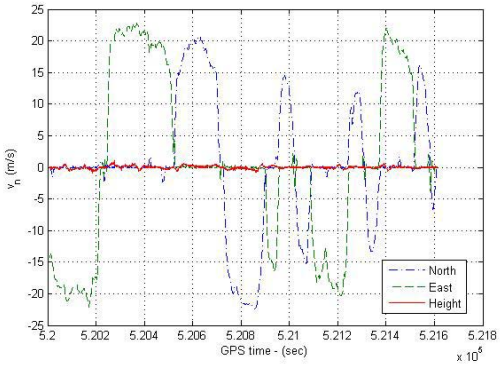


Fig. 3. Velocity of the field test.

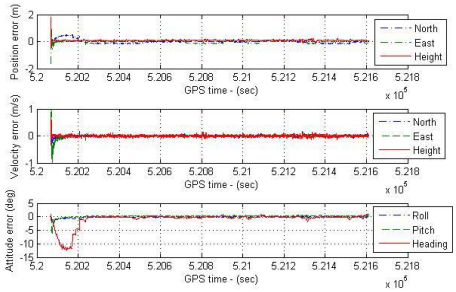


Fig. 4. Error of MEMS/DGPS navigation using DGPS heading and innovation detection.

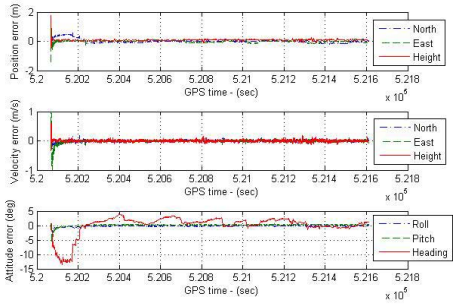


Fig. 5. Error of MEMS/DGPS navigation without using DGPS heading.

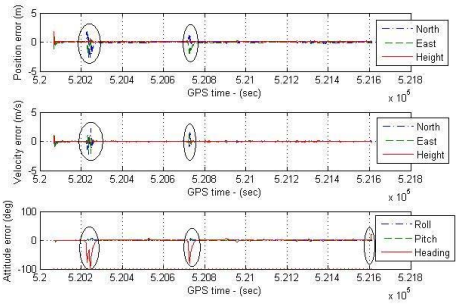


Fig. 6. Error of MEMS/DGPS navigation using DGPS heading without innovation detection.

TABLE I
RMS ERRORS

| | Using DGPS Heading and Innovation Detection | Without Using DGPS Heading | Using DGPS Heading without Innovation Detection |
|---|---|---|---|
| Roll (deg) | 0.10193 | 0.11003 | 0.68784 |
| Pitch (deg) | 0.10128 | 0.09911 | 0.35197 |
| Heading (deg) | 0.30887 | 1.16086 | 6.26533 |
| North Velocity (m/s) | 0.023 | 0.024 | 0.067 |
| East Velocity (m/s) | 0.020 | 0.021 | 0.068 |
| Height Velocity (m/s) | 0.029 | 0.029 | 0.033 |
| North (m) | 0.090 | 0.071 | 0.111 |
| East (m) | 0.091 | 0.069 | 0.167 |
| Height (m) | 0.088 | 0.088 | 0.096 |

## VI. CONCLUSION

The heading accuracy of MEMS IMU/DGPS integrated navigation system will be decreased significantly fast with time when the vehicle moves along a straight road with no or small change in its attitude and acceleration. In order to overcome this problem, a new heading measurement derived from DPGS position is introduced to improve the heading accuracy. A sequential Kalman filter is presented to implement the MEMS IMU/DGPS integrated navigation system. In order to deal with singular DGPS heading measurements, an innovation detection method is used to detect and reject the singular heading measurement. The field test results show that the heading accuracy can be improved significantly by using the heading measurement derived from DGPS position. The results also show that the singular DGPS heading measurements can be detected and rejected effectively by the method of the innovation detection. The method investigated in this paper can significantly improve the heading accuracy of MEMS/DGPS integrated navigation in land vehicle applications, and effectively handle the occurrences of singular heading measurements when the vehicle makes turns.

## ACKNOWLEDGEMENT

This study was supported in part by research fund from the Natural Science and Engineering Research Council of Canada (NSERC) and Geomatics for Informed Decisions (GEOIDE), Network Centers of Excellence (NCE) to Dr. Naser El-Sheimy.

## REFERENCE

[1] S. Hong, M. H. Lee, J. A. Rios and J. L. Speyer, "Observability Analysis of INS with a GPS Multi-antenna System*", Korean Society of Mechanical Engineers International Journal*, vol. 16, no. 11, pp. 1367-1378, 2002.

[2] Hong, M. H. Lee, H. Chun, S. Kwon and J. L. Speyer, "Observability of Error States in GPS/INS Integration", *IEEE Tansactions on Vehicle Technology*, vol. 54, No. 2, pp. 731-743, 2005.

[3] E. H. Shin, *Estimation Techniques for Low-Cost Inertial Navigation*. PhD Thesis, MMSS Research Group, Department of Geomatics Engineering, University of Calgary, Calgary, Alberta, Canada, UCGE Report No. 20219, 2005.

[4] Mohinder S. G. and Angus P. A., *Kalman Filtering: Theory and Practice Using MATLAB*, Second Edition, John Wiley & Sons, Inc., New York, 2001.

[5] H. E. Rauch, F. Tung, and C. T. Striebel, "Maximum likelihood estimates of linear dynamic systems," *J. Amer. Inst. Aeronaut. Astronauts*, vol. 3, no. 8, pp. 1445–50, 1965.